Supporting Information

coordinates of the active site as used in the calculations
positions of non-hydrogen atoms taken from the X-ray structure

H	-0.717	-5.695	0.922
C	-1.037	-4.656	0.976
N	-1.135	-4.242	2.372
H	-2.024	-4.221	2.781
C	-0.098	-3.889	3.123
N	1.131	-3.882	2.618
H	1.282	-4.143	1.665
H	1.905	-3.616	3.192
N	-0.287	-3.591	4.401
H	-1.206	-3.632	4.793
H	0.490	-3.325	4.972
H	1.075	3.797	-0.716
C	0.759	2.757	-0.774
S	0.010	2.149	0.777
H	3.616	-0.720	1.334
C	3.167	-1.338	0.558
S	2.171	-0.443	-0.680
H	-4.215	-1.135	0.330
C	-3.134	-1.255	0.242
S	-2.272	0.325	0.373
H	-2.006	0.844	-3.627
C	-1.660	-0.044	-3.099
S	0.000	0.000	-2.374
Fe	0.900	-2.126	-1.776
Ni	0.000	0.000	0.000
C	-0.500	-2.802	-2.179
N	-1.352	-3.498	-2.667
C	1.724	-3.608	-0.969
N	2.323	-4.567	-0.538
C	1.695	-2.164	-3.124
O	2.251	-2.621	-4.094
O	0.000	-1.772	0.180
H	0.025	2.661	-1.575
H	1.630	2.142	-1.003
H	3.971	-1.855	0.032
H	2.522	-2.070	1.044
H	-2.786	-1.915	1.037
H	-2.907	-1.702	-0.726
H	-2.364	-0.237	-2.290
H	-1.684	-0.874	-3.807
H	-0.311	-4.026	0.462
H	-2.012	-4.552	0.498
C	4.223	1.734	-5.191
C	3.525	1.589	-4.039
N	3.468	1.130	-6.171
C	2.359	0.644	-5.634
N	2.373	0.911	-4.343
H	1.634	0.159	-6.124
H	3.800	1.916	-3.134
H	5.107	2.188	-5.306

coordinates of model **1'**
optimized (basis set A and VWN functional)
coordinate system oriented along the g-tensor axes

H	1.701	5.353	1.465
C	1.817	4.273	1.393
N	1.808	3.685	2.729
H	2.669	3.448	3.130
C	0.708	3.450	3.436
N	-0.490	3.736	2.938
H	-0.570	4.132	2.024
H	-1.311	3.556	3.478
N	0.813	2.972	4.668
H	1.715	2.791	5.059
H	-0.012	2.793	5.206
H	-1.822	-3.364	-1.293
C	-1.314	-2.403	-1.227
S	-0.573	-2.089	0.457
H	-3.502	1.279	1.292
C	-2.930	1.888	0.595
S	-2.122	0.824	-0.663
H	4.283	0.314	0.319
C	3.247	0.646	0.250
S	2.053	-0.841	0.253
H	1.818	-0.727	-3.839
C	1.636	0.142	-3.208
S	-0.039	0.243	-2.426
Fe	-0.599	2.342	-1.516
Ni	0.000	0.000	0.000
C	0.925	3.107	-2.030
N	1.978	3.515	-2.363
C	-1.180	3.973	-0.657
N	-1.469	5.004	-0.109
C	-1.256	2.849	-2.967
O	-1.697	3.515	-3.873
O	0.380	1.851	0.156
H	1.332	1.997	-0.102
H	-0.560	-2.355	-2.013
H	-2.048	-1.611	-1.378
H	-3.611	2.607	0.137
H	-2.166	2.421	1.163
H	3.015	1.262	1.119
H	3.127	1.240	-0.657
H	2.348	0.100	-2.384
H	1.830	1.030	-3.811
H	0.995	3.858	0.810
H	2.764	4.043	0.903
C	-4.435	-0.225	-5.478
C	-3.758	-0.370	-4.277
N	-3.614	0.345	-6.431
C	-2.439	0.548	-5.818
N	-2.495	0.123	-4.520
H	-1.714	0.159	-3.823
H	-1.559	1.009	-6.255
H	-4.050	-0.746	-3.300
H	-5.465	-0.486	-5.703

coordinates of model **2b'**
optimized (basis set A and VWN functional)
coordinate system oriented along the g-tensor axes

H	0.071	5.695	0.950
C	0.535	4.712	0.907
N	0.888	4.273	2.253
H	1.820	4.367	2.535
C	0.027	3.752	3.121
N	-1.248	3.584	2.789
H	-1.568	3.850	1.880
H	-1.888	3.192	3.449
N	0.436	3.445	4.344
H	1.387	3.605	4.608
H	-0.207	3.052	5.002
H	-0.611	-3.900	-0.907
C	-0.453	-2.825	-0.955
S	0.273	-2.105	0.601
H	-3.432	0.139	1.699
C	-3.187	0.839	0.901
S	-2.248	-0.003	-0.420
H	4.042	1.705	-0.346
C	2.954	1.672	-0.279
S	2.256	-0.089	-0.196
H	2.717	-0.456	1.069
H	1.586	-0.447	-4.059
C	1.200	0.365	-3.444
S	-0.318	-0.006	-2.451
Fe	-1.418	1.834	-1.523
Ni	0.000	0.000	0.000
C	-0.302	3.023	-2.271
N	0.483	3.724	-2.799
C	-2.425	3.258	-0.670
N	-2.962	4.188	-0.135
C	-2.384	1.981	-2.901
O	-3.131	2.383	-3.762
O	-0.217	1.876	0.070
H	0.574	2.351	-0.309
H	0.139	-2.599	-1.843
H	-1.424	-2.334	-1.031
H	-4.122	1.251	0.517
H	-2.586	1.641	1.330
H	2.636	2.250	0.588
H	2.532	2.111	-1.183
H	1.979	0.632	-2.730
H	1.008	1.212	-4.106
H	-0.163	4.000	0.466
H	1.437	4.764	0.295
C	-4.620	-2.174	-4.798
C	-3.800	-1.951	-3.706
N	-4.156	-1.468	-5.903
C	-3.067	-0.820	-5.485
N	-2.822	-1.091	-4.166
H	-2.021	-0.745	-3.607
H	-2.455	-0.147	-6.080
H	-3.831	-2.298	-2.678
H	-5.511	-2.790	-4.858

Table S1. Interatomic Distances of Active Site Models Including Arg463 and His72 (protonated at Nε), compared to XRD data

	interatomic distances [Å][a]								
structure	Ni-Fe	Ni-O	Ni-S65	Ni-S68	Ni-S530	Ni-S533	Fe-O	Fe-S68	Fe-S533
1'	2.85	1.90	2.21	2.37	2.23	2.44	2.00	2.31	2.35
2a'	2.80	1.86	2.23	2.34	2.23	2.46	1.99	2.31	2.34
2b'	2.77	1.89	2.21	2.29	2.27	2.47	2.00	2.30	2.34
3'	2.80	1.80	2.27	2.37	2.24	2.60	1.88	2.35	2.44
Ni-A[b]	2.9 (2.9)	1.8 (1.9)	2.3 (2.2)	2.3 (2.5)	2.3 (2.3)	2.4 (2.5)	2.2 (2.2)	2.4 (2.3)	2.4 (2.3)

[a] Values taken from spin-restricted calculations with basis set A and the VWN functional. [b] Values taken from two different refinements of crystallographic data of the *D. fructosovorans* mutant (see Table 1).

Discussion of experimental and computed hyperfine coupling values

Direct comparison of calculated and experimental values is not always possible, particularly when the latter were taken from simple EPR spectra, either directly or by simulation of experimental spectra. Most frequently, experimental A_i values are obtained from simulations of randomly oriented systems within the assumption of parallel g- and A-tensor axes. However, this may lead to significant errors if the axes actually are not coincident, which is always the case when systems of low symmetry are studied: the values A_i obtained when carrying out such a simulation are not identical with the tensor's principal values, although the simulated spectrum might fit the experimental one very well. We illustrate this in Figures A and B where two simulated EPR spectra are compared.

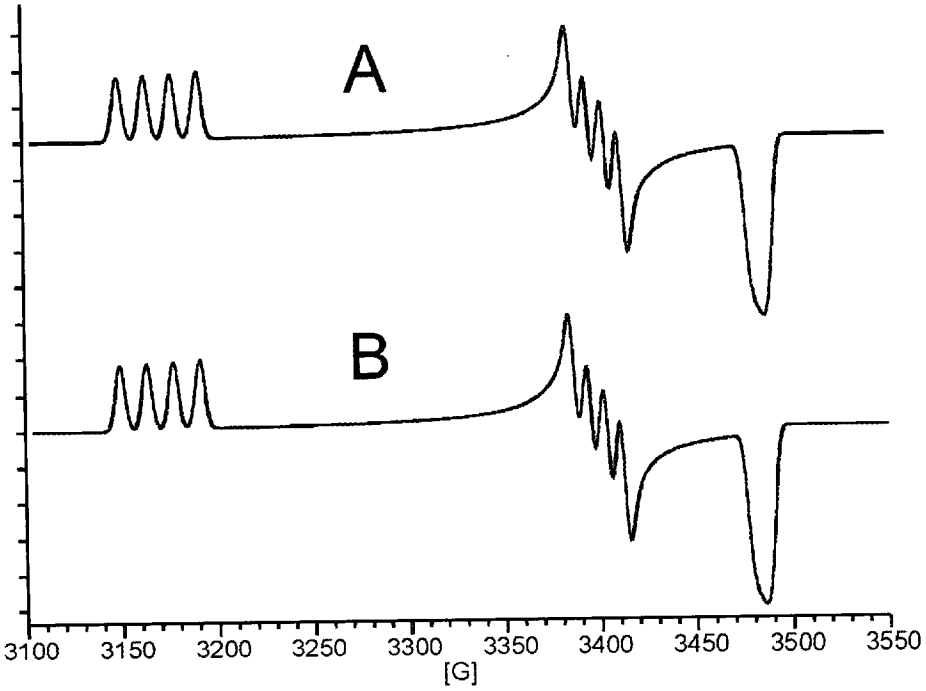

We have chosen a spin doublet system that shows hyperfine coupling to one nucleus with spin 3/2 (i.e. ^{61}Ni), which is a rather simple system and similar to those discussed in this and the accompanying paper. In Figure A, which represents a fictitious "experimental" spectrum, the orientation of the A-tensor, with principal values $A(1, 2, 3) = (50.0, 0.0, 10.0)$ MHz, is such that A_3 is parallel to g_z whereas the angle between A_1 and g_x is 30°. Figure B shows an attempt to simulate that same spectrum, assuming essentially parallel tensors and adjusting the three A_i principal values for optimal agreement with spectrum A. Obviously, the latter is simulated quite well, but within the assumption of parallel tensors the principal values now need to be $A(1, 2, 3) = (\pm 43, \pm 25, \pm 10)$ MHz. This corresponds to $a_{iso} = \pm 26$ MHz if equal signs are chosen for the three components whereas the value of a_{iso} in Figure A in fact is 20 MHz. This demonstrates very clearly that in cases with non-coincident axes the simulation of EPR (and sometimes even ENDOR) spectra, if this non-coincidence is not considered, may yield principal values A_i and, consequently, values of T_i and a_{iso} that are not correct.

In our example one axis of the A-tensor was still parallel to the corresponding g-tensor axis. If none of the axes coincide, which is always the case in systems without symmetry, the deviation from the real values may be even bigger. This is a problem that must always be kept in mind when discussing the hyperfine interactions in hydrogenases.

Table S2. Hyperfine Couplings Computed for Active Site Models Including Arg463, His72 (protonated at Nε) and Dielectric Effects[a,b]

		hyperfine coupling [MHz]					
structure		^{61}Ni	^{57}Fe	^{17}O	^{33}S (Cys533)	^{1}H$_1$ (Cys533)	^{1}H$_2$ (Cys533)
1'	a_{iso}[c]	-16.2	-0.6	-3.2	35	20	15
	T(1,2,3)[d]	(*27*, *6*, -33)	(*-1*, *0*, *1*)	(6, *-8*, *2*)	(*-23*, *-21*, *44*)	(*3.5*, -2.9, *-0.6*)	(*-1.1*, *-1.7*, *2.8*)
2a'	a_{iso}[c]	2.5	-0.7	-4.6	30	25	16
	T(1,2,3)[d]	(*34*, *4*, -38)	(*2*, *-2*, *0*)	(8, *-12*, *4*)	(*-26*, *-24*, *50*)	(*3.4*,*-3.1*, *-0.4*)	(*-1.1*, *-1.9*, *3.0*)
2b'	a_{iso}[c]	-13.3	-0.8	-2.8	25	26	23
	T(1,2,3)[d]	(*-7*, *40*, -33)	(*-4*, *2*, *2*)	(*5*, *2*, *-7*)	(*-27*, *-24*, *51*)	(*3.8*, *-2.8*, *-1.0*)	(*-1.1*, *-2.0*, *3.1*)
3'	a_{iso}[c]	-6.8	-1.0	-14.6	34	13	6
Ni-A	a_{iso}	–	~ $\underline{1}$[27a]	11[29]	–	–	–
	A(1,2,3)	($\underline{24}$, $\underline{47}$, $\underline{76}$)[30a]	–	±(5, 7, 20)[29]	–	($\underline{13}$, –, –)[32a]	($\underline{13}$, –, –)[32a]
Ni-B	a_{iso}	–	< $\underline{1}$[27a]	–	–	12.6[32b]	12.5[32b]
	T(1,2,3)	–	–	–	–	(-1.8, -2.4, 4.2)[32b]	(-1.4, -1.4, 2.8)[32b]
	A(1,2,3)	–	–	–	($\underline{31}$, $\underline{42}$, –)[31]	($\underline{15}$, –, –)[32a]	($\underline{15}$, –, –)[32a]

[a]Dielectric effects were modeled with COSMO using the dielectric constant ε = 4.
[b]Underlined numbers indicate that the sign could not be determined. An italicized number indicates that the axis of the calculated T- or A-tensor does not coincide (not even approximately) with the corresponding g-tensor axis.
[c]Values taken from spin-unrestricted calculations using basis set B' (for Ni, Fe, O, S and Nε) and BP gradient correction.
[d]Values taken from spin-restricted spin-orbit calculations with basis set A and BP gradient correction.

^{61}Ni (only Ni-A): For model **1'** the calculations indicate that the z-axis of the A-tensor is (almost) parallel to the corresponding g-tensor axis g_z whereas the angle between A_1 and g_x (and also between A_2 and g_y) is about 30°. Thus, direct comparison with available experimental data is difficult for A_1 and A_2 but not for A_3. However, Table S2 demonstrates that A_3 is calculated much too small, the combination of calculated values a_{iso} and T_3 yielding A_3 = -49 MHz. Closer inspection indicates that this is mainly due to an incorrect value a_{iso} (-16 MHz using basis set B' and -14 MHz using the basis set of Stein et al. [Ref. 10 in the accompanying work]): simulation of EPR spectra gives acceptable results if we combine the calculated T-tensor with a_{iso} = -47±2 MHz, which is our rough estimate of the (undetermined) experimental value a_{iso} assuming negative signs for all three principal values of the A-tensor. Therefore, we conclude that the T-tensor is well calculated whereas a_{iso}^{calc} is about three times smaller than a_{iso}^{exptl}. For the oxo-bridged model **3'** agreement between calculated and estimated experimental values a_{iso} is even worse than for model **1'**, and the same can be said about the T-tensors of models **2a'** and **2b'**, strongly favoring model **1'** as candidate for Ni-A.

^{57}Fe: In ^{57}Fe ENDOR experiments the hyperfine interaction with Fe was too small to be detected in Ni-B whereas it could be measured in Ni-A, being roughly isotropic with a_{iso}(^{57}Fe) ≈ 1 MHz. [Ref. 27a] Considering the accuracy of our method all models in Table S2 are in reasonable agreement with the experimental data of Ni-A and possibly also with those of Ni-B. Unfortunately, the experimental finding of a smaller coupling in Ni-B is not reproduced by our favorite Ni-A and Ni-B models **1'** and **2b'**, respectively. It should be noted, however, that the experiments were performed on hydrogenases from two different enzymes, i.e. Ni-A from *D. gigas* and Ni-B from *Desulfovibrio desulfuricans*, and that the A-tensor of Ni-B was not fully characterized. Moreover, in Ni-C also no hyperfine coupling with ^{57}Fe was detected originally

[Ref. 27a] but very recently this result had to be corrected. [Ref. 29] Without doubt, additional experimental data are required to unambiguously resolve these problems.

^{17}O: Very recently for Ni-A the orientation of the A-tensor has been shown to be rotated relative to the g-tensor by an angle of about 45° about the common (g_1, A_1) axis [Ref. 29], which is exactly what our calculations of model **1'** predicted. If we now assume that the isotropic component is about three times bigger than our calculated value (in accordance with the experimental value of 11 MHz) and if we use the calculated T-tensor in Table S2 we obtain an A-tensor that agrees almost perfectly with the experimental one, except for the signs. In fact, we then obtain (-4, -18, -8) MHz but due to the mentioned angle of 45° this yields practically the same spectra as a simulation with the experimentally determined values. It should also be noted that simulation of a simple EPR spectrum agrees very well with a spectrum of ^{17}O containing Ni-A recorded fifteen years ago by Cammack and Fernández (unpublished). All this indicates that the T-tensor is rather well calculated for model **1'**. For model **3'** simulation is not meaningful because the calculated T-tensor cannot be trusted.

We would like to note that the broadening of EPR lines due to the presence of ^{17}O in the Ni-A and Ni-B states of *C. vinosum* hydrogenase reported by van der Zwaan et al. [Ref. 28] is not very useful for further verification of our models. Their experimental data indicate that the hyperfine coupling is practically isotropic in Ni-A but rather anisotropic in Ni-B. At least for Ni-A, this is in complete disagreement with the above mentioned data obtained from *D. gigas* hydrogenase and also with those calculated for model **1'**. It can not be excluded that this is due to structural differences between the hydrogenases from these two organisms. However, the available data indicate that the magnitude of the hyperfine coupling is similar in Ni-A and Ni-B and, thus, the big difference between the calculated values a_{iso} of model **1'** and **3'** makes it rather unlikely that they correspond to these two enzyme states.

^{33}S (only Ni-B): The available experimental data for the ^{33}S coupling are not sufficient to verify our computational models. Moreover, the calculated values are rather similar for all four models listed in Table S2.

^{1}H: The only proton hyperfine principal values that in principle can be compared directly with experimentally determined values are those of the two protons at Cβ of Cys533 in Ni-B since only the signals of these two protons could be assigned with certainty. [Ref. 32b] Unfortunately, there are serious difficulties for understanding the orientation of the A-tensors of these two protons as reported by Gessner et al. [Ref. 32b] The given Euler angles describing the relative orientation of g- and A-tensor principal axes are not in agreement with our calculation although the relative atomic positions of Ni and the two protons and the orientation of the g-tensor, which are the main factors controlling the A-tensor anisotropy, are rather similar. Consequently, for proton H_1 the assignment of experimental and calculated values T_1, T_2 and T_3 in Table S2 seems to be completely different, which seems rather unreasonable from our point of view. In fact, rather good agreement between calculation and experiment, particularly for model **2b'**, is found if the experimental values T_1 and T_3 are swapped. This would also put in agreement the experimental values for A_1 given in Refs. 32a and 32b. On the other hand, for the T-tensor of proton H_2 the best agreement is found for model **1'**. In fact, no preference can be made on this basis between models **1'** and **2'** because the deviation from experiment is bigger than the observed differences among the different computational models.

Analysis of the isotropic components does not really clarify the situation. They are generally calculated too big. Whereas experimentally both protons show practically the same coupling, the calculated values are significantly different. This is most pronounced for model **2a'** confirming that model **2b'** is a better Ni-B model. It should be noted that the values a_{iso} for

H_1 and H_2 are even more different when the *basic model* is used (data not shown), demonstrating that the electronic structure is better described including the imidazole group and dielectric effects. On the other hand, the results obtained with the *extended model* can still be improved by modeling Cys533 as S-CH_2-CH_3, e.g. for Ni-A model **1'** values of 16 and 15 MHz are computed for a_{iso} of H_1 and H_2, respectively. Apparently, new experimental results indicate that the isotropic hyperfine coupling of both protons is somewhat smaller in Ni-A than in Ni-B (see Ref. 7i). This is exactly what our calculations predicted.